Journal of Materials Chemistry A

Accepted Manuscript

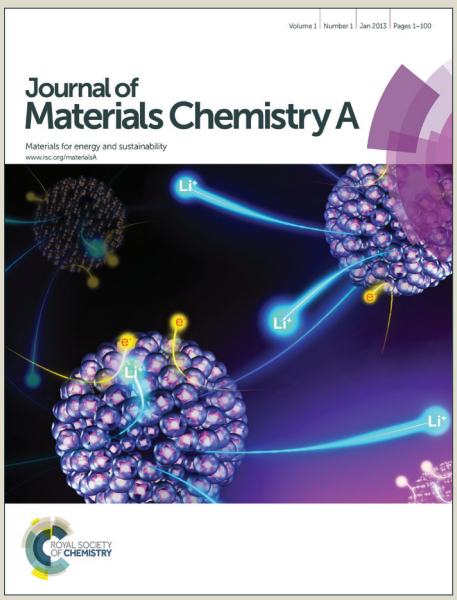

ROYAL SOCIETY OF CHEMISTRY

www.rsc.org/materialsA

Facile Fabrication of Stable Monolayer and Few-layer Graphene Nanosheets as Superior Sorbents for Persistent Aromatic Pollutant Management in Water

Kaijie Yang,[ab] Jun Wang,[ab] and Baoliang Chen [*ab]

[a] Department of Environmental Science, Zhejiang University, Hangzhou 310058, China

[b] Zhejiang Provincial Key Laboratory of Organic Pollution Process and Control, Hangzhou 310058, China

* Corresponding Author E-mail: blchen@zju.edu.cn

Phone: 0086-571-88982587

Fax: 0086-571-88982587

Table of Content (TOC)

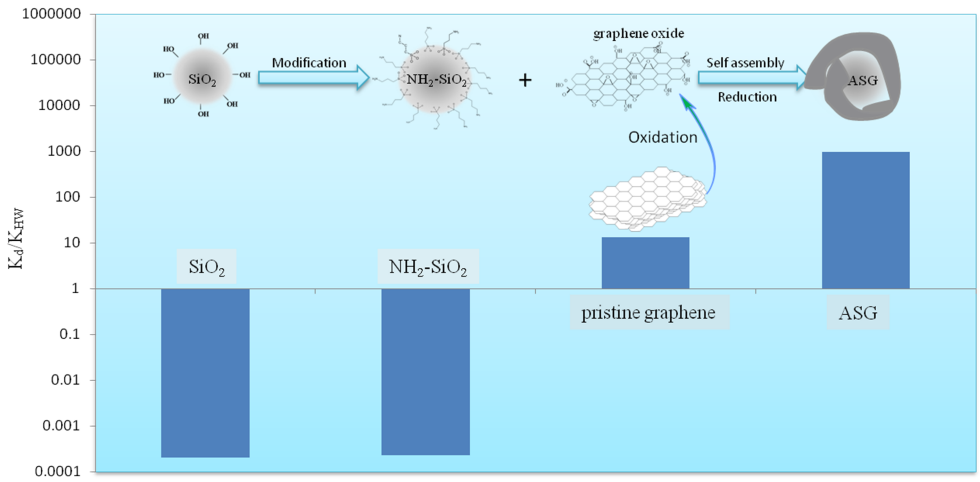

Abstract

A facile method was employed to prepare stable monolayer and few-layer graphene (ASG) nanosheets by loading on nanosilica substrates. The adsorption capability of ASG was enhanced by a factor of up to 10^2 for phenanthrene compared with pristine graphene, which was higher than that in previous reports for nanomaterials. Interaction mechanisms of monolayer graphene with organic solute were discussed.

Introduction

Graphene is a 2D, single-atom thick carbon sheet with the carbon atoms arranged in a honeycomb pattern.[1] Its discovery has attracted enormous attention because of its remarkable electronic properties, ultra strong mechanical strength, optical transmittance and large surface area, which are important for various applications, including energy storage,[2] catalysis,[3] electronics,[4] sensing,[5,6] biointerface transport [7,8] and environmental pollution management.[9-19] The majority of chemical and biological processes in the environment and in biology occur at the liquid/solid interface of monolayer graphene/water systems.[5,8,11,17] However, it is a critical challenge to obtain stable monolayer graphene sheets in water for investigating nanoscale interactions with organic solutes on the graphene plane because significant aggregation of the nanosheets occurs via large area π-π interactions and strong van der Waals forces.[11,12,17] Furthermore, the aggregation hides the huge surface area of graphene nanosheets,[11] and then may hinder the adsorption capability of graphene to environmental pollutants.[16] Therefore, most knowledge on the adsorption capacity of graphene in aqueous solutions has been obtained from pristine stacked graphene,[10-13,20] and the largely microscopic mechanisms have been derived from theoretical simulations.[21] Thus, the true adsorption potential of monolayer

graphene remains poorly understood. Moreover, the mechanism determined via theoretical simulations must be verified by experimental methods. Herein, we report a facile method to prepare stable monolayer and few-layer graphene in water by controlling the loading of graphene on nanosilica (nano-SiO_2) as a framework, reveal the truly powerful adsorption potential of graphene, and provide insight on nanoscale interactions between monolayer graphene and organic solutes at the water/solid interface.

Results and discussion

In this study, a facile and low-cost approach to stabilize monolayer and few-layer graphene in water was employed using a core-shell structure (SiO_2@graphene). Nanosilica was selected because of its considerable realistic significance due to the unavoidable interaction between graphene and silica when graphene is discharged into environments where silica is widespread. The fabrication progress is presented in Figure 1. Briefly, the supporting SiO_2 was first modified with 3-aminopropyltriethoxysilane (APTES) to bind with $–NH_2$ and make it positively charged. Monolayer graphene oxide (GO) was synthesized using the modified Hummer's method followed by ultrasonication.[22,23] The self-assembly between GO and aminosilica (NH_2-SiO_2) was conducted at proper pH conditions and controlled concentrations under mechanical stirring. After obtaining the aminosilica-support-graphene oxide (ASGO), aminosilica-support-graphene (ASG) was produced by traditional chemical reduction. The detailed process of the fabrication, structural characterization, and adsorption experiments are presented in the electronic supplementary information (ESI).

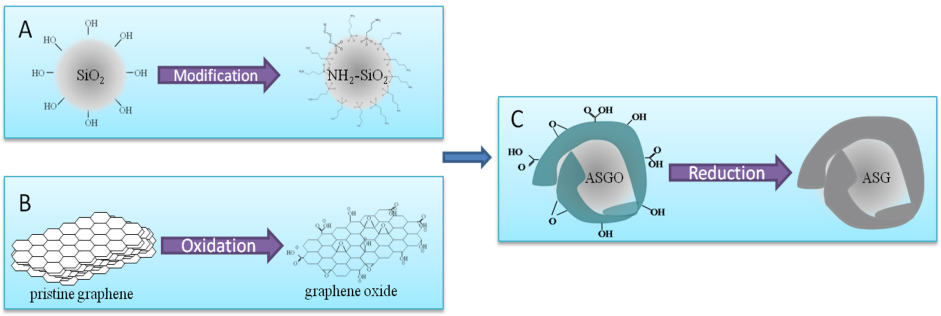

Figure 1. The chemical route for the fabrication of aminosilica-support-graphene (ASG). (A) Modification of SiO_2 with $–NH_2$. (B) Cleavage graphene nanosheets via oxidation. (C) Coating of negative charged graphene oxide on the positive charged NH_2-SiO_2, and then conversion to ASG via chemical reduction.

The prepared products were analyzed by Fourier transform infrared spectroscopy (FTIR) (Figure S-1). Two additional adsorption peaks appeared in NH_2-SiO_2 at 2854 and 2926 cm^{-1}, which were assigned to the C-H vibration of the grafted APTES, indicating the successful synthesis of NH_2-SiO_2. The elemental analysis results (see Table S-1 in ESI) suggested that NH_2-SiO_2 had an additional N percentage of 0.4258% compared with SiO_2. The surface area (Table S-2) and zeta potential (Figure S-2) of NH_2-SiO_2 and GO were measured to verify the appropriate fabrication conditions. NH_2-SiO_2 had a surface area of 108.5 m^2/g. Through theoretical calculations, one gram of NH_2-SiO_2 can completely support 41.25 mg of graphene (2630 m^2/g) in a monolayer state at full coverage. To supply sufficient loading regions on the NH_2-SiO_2 during fabrication, the proportion of graphene in ASG was maintained below 4.13%. From the zeta potential analysis, NH_2-SiO_2 and GO were oppositely charged in the pH range from 1 to 8; thus, the GO and aminosilica (NH_2-SiO_2) were able to self-assemble via electrostatic interactions. Once attached, the positive charges on the surface of NH_2-SiO_2 were neutralized by the negatively charged graphene. After coating with monolayer GO nanosheets,

no additional GO sheets could bind to the surface of SiO_2 due to the electrostatic repulsion between the adlayer GO and the free GO. In addition, the disappearance of the FTIR peak for C=O (1725 cm^{-1}) in ASGO compared with GO suggested the occurrence of a chemical reaction between –COOH and -NH_2. The final product of ASG was obtained through the chemical reduction of ASGO. The surface charge of ASG was highly positive (Figure S-2) and was dominated by the core of NH_2-SiO_2 rather than by the outer region of the graphene adlayer. Even under ultrasonication conditions, no graphene nanosheets dissolved from the ASG, suggesting that the combination of graphene and NH_2-SiO_2 was stable.

The microstructures of the pristine as-prepared graphene and ASG were examined by SEM and HR-TEM. The SEM image (Figure 2A) indicates that the pristine graphene was seriously assembled, as reported.[11,12] After wrapping the surface of the NH_2-SiO_2, the stacked interlamination was loosened, and the morphology was fluffy and porous (Figure 2B) due to the electrostatic repulsion between the positively charged ASG particles. The large area face-to-face interaction between the graphene nanosheets caused by the π-π interactions and van der Waals forces was transformed into a point-to-point interaction with the support of SiO_2. In addition, the ASG exhibited a core-shell structure of SiO_2@graphene with an ultrathin graphene layer (Figure 2C), which was confirmed by HR-TEM (Figures 2D and 2E). From the AFM images (Figure 2G-2H) and Raman spectra (Figure 2F), we observed that the graphene layer loading on the surface of SiO_2 was only a few layers or even a monolayer. Because of the large area of the graphene sheet, part of the graphene layer extended outside the edge of the SiO_2 (Figure 2E). As reflected in the AFM image, the height of the extended graphene was approximately 2 nm, as observed in Figure 2(I_1), representing approximately

two or three layers of overlapped, extended graphene.[24-27] In some areas, the height of the extended graphene layer was only 0.5 nm (Figure 2I$_1$), which was nearly equal to the theoretical thickness of monolayer graphene (0.34 nm).[26] In the Raman spectra (Figure S-3), the 2D peak of ASG exhibited an obvious down-shift compared with pristine graphene (Figure 2F), which also demonstrated that the graphene nanosheets in the ASG comprised less than 5 layers or even only a monolayer.[25,28] The size of the ASG particle was approximately 100 nm (Figures 2C and 2I$_2$).

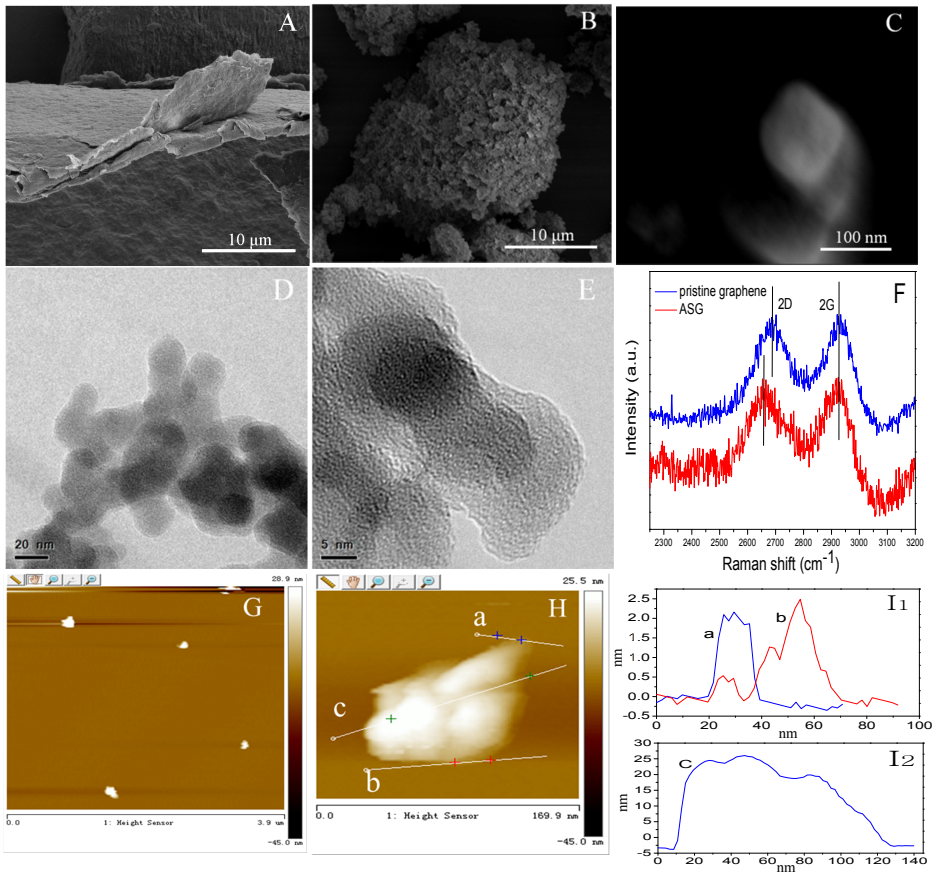

Figure 2. SEM images of pristine graphene sheets (A), the ASG bulk view (B) and an ASG single particle (C). HR-TEM images of the ASG in bulk view (D) and at high magnification (E). 2D peak in the Raman spectra of the ASG and of pristine graphene (F). AFM images showing a bulk view (G) and a single ASG particle (H). The height of each testing line in Figure (H) was presented in Figure (I$_1$) and Figure (I$_2$).

To probe the superior adsorption capacity of the monolayer and few-layer graphene nanosheets, batch tests of the adsorption performance were conducted to determine the adsorption capability of SiO_2, NH_2-SiO_2, ASG and pristine graphene (Figure 3). Phenanthrene was selected as a model solute because it is a typical persistent organic pollutant. The isotherms of SiO_2, NH_2-SiO_2, ASG and pristine graphene were further fitted by Freundlich model (the regression parameters are presented in Table S-3). The clear structure only containing three benzenes without other complex groups indicates that the interactions between the graphene nanosheets and phenanthrene should consist of no more than the hydrophobic effect and π-π interactions.[11,29] The rapid equilibration (60 min) (Figure S-4) illustrated the high adsorption efficiency of this material. Clearly, the phenanthrene adsorption to SiO_2 and NH_2-SiO_2, which possess hydrophilic surfaces, was extremely low. Notably, once the silica materials were wrapped by the monolayer and few-layer graphene nanosheets (the content of graphene was only 0.5876%), the phenanthrene adsorption capacity improved sharply, by a factor of up to 3×10^4. The graphene sheets, in a manner similar to a large cloth, tightly attached to the surface of SiO_2 (Figures 2E and 2H), which transformed the hydrophilic interface of SiO_2 into an aromatic hydrophobic interface. The interaction mechanism with phenanthrene was therefore altered. As SiO_2 is widely existed in the environment, simple combination of released graphene and SiO_2 will dramatically improve the adsorption capacity of SiO_2 with environmental pollutants. The resulting drastic change will deeply effect the fate and transport of pollutants in the environment, which may be then aggravated environmental risks of the released graphene.

The adsorption capacities with different adsorbents by mass are presented in Figure 3A. Obviously, the adsorption capacity of ASG is lower than the pure pristine graphene, because

SiO_2 has little affinity to phenanthrene and the content of graphene is just 0.5876%. During fabrication, SiO_2 was added as auxiliary material to excavate the potential capacity of graphene. For ASG, the well-dispersed graphene nanosheets displayed a large improvement, by a factor of up to 10^2, in adsorption quantity compared with agglomerated graphene for the same graphene content (Figure 3B). The monolayer and few-layer graphene nanosheets

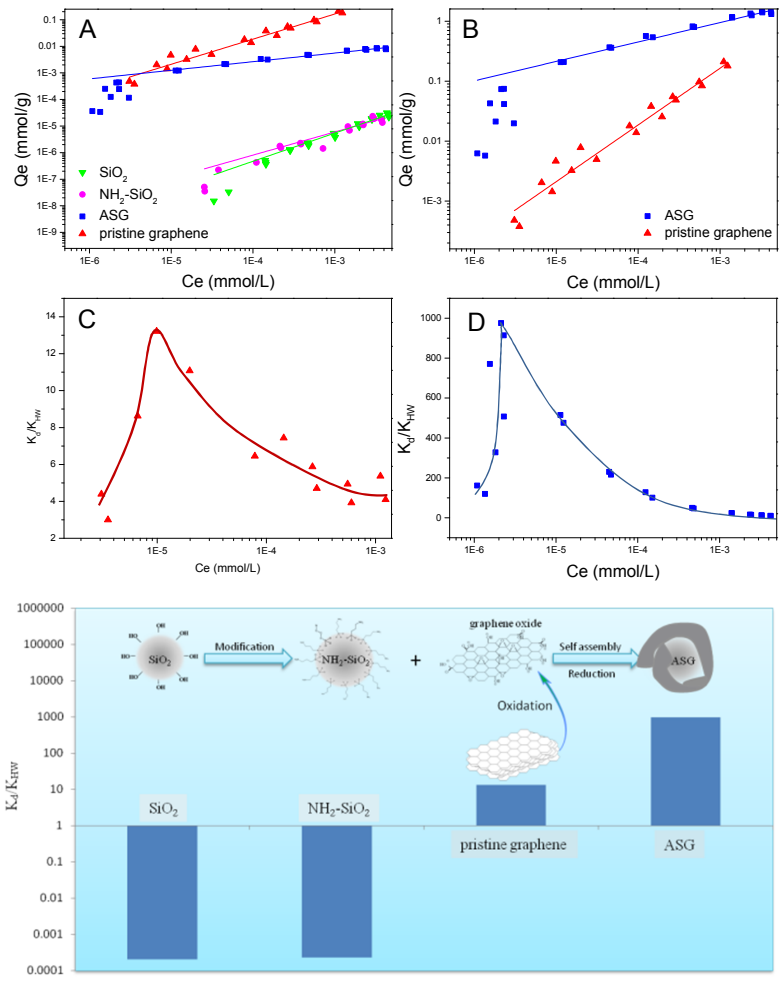

Figure 3. Adsorption isotherms of phenanthrene on SiO_2, NH_2-SiO_2, ASG and pristine graphene (A). Comparative adsorption capacity of ASG and pristine graphene at the same graphene content (B). The variation curves of K_d/K_{HW} of pristine graphene (C) and ASG (D) with equilibrium concentrations of phenanthrene. The maximum values of the K_d/K_{HW} ratio for phenanthrene adsorption to various materials (E). The initial concentration of phenanthrene ranged from 0.0056 to 0.56 μmol/L. The water-to-solid ratio was 200 mg/8 mL for SiO_2, 200 mg/8 mL for NH_2-SiO_2, 1 mg/240 mL for pristine graphene, and 1 mg/8 mL for ASG.

exhibited superior adsorption performance for phenanthrene, with capacities of up to 1.43 mmol/g. We ascribe this strong adsorption capability to two sources: (1) Graphene aggregation was avoided, and the graphene was present as monolayer and few-layer graphene on an nano-SiO_2 support. After that, the abundance of potential active adsorption sites of the pristine graphene, which were concealed on the inner sheets and occupied by interfacial water molecules,[26] were released and functioned as superior affinity regions. (2) There are two adsorption sites on the graphene ad-layer, i.e., the flat surface and the grooves.[11,29] A groove is a high surface energy site, and molecules will prefer to adsorb to the groove, while the flat surface remains unoccupied. Benefitting from the rugged surface of the monolayer graphene on nano-SiO_2, many additional wrinkles will be created to form large and powerful groove regions in a stable state.[30,31]

To gain further insight into the adsorption mechanism, the hexadecane-water partition coefficient (K_{HW}=34581 L/kg for phenanthrene) was introduced to highlight the interaction strength beyond the hydrophobic effect.[32] K_{HW} has been widely used as a surrogate for modeling the transport and partition of organic molecules on biological interfaces.[33] As observed in Figure 3C, the affinity of the organic solute to pristine graphene was much higher than K_{HW}, and the peak K_d/K_{HW} ratio was as high as 13 at the phenanthrene equilibrium concentration (C_e) of 1.2×10^{-5} mmol/L. The affinity of the monolayer and few-layer graphene nanosheets was much higher than K_{HW}, and the maximum K_d/K_{HW} reached 1,000 at C_e = 2.4×10^{-6} mmol/L (Figure 3D). That is, the enrichment capacity of the monolayer and few-layer graphene was 10^3 times higher than that of hexadecane, which acted as a surrogate phospholipid bilayer. These data are much higher than the K_d/K_{HW} ratio of naphthalene on

sulfonated graphene, which has beeb one of the highest adsorption capabilities reported for nanomaterials.[17] Compared with SiO_2, NH_2-SiO_2 and pristine graphene, the monolayer and few-layer graphene loading on nanosilica acted as a superior sorbent for persistent aromatic organic pollutants in water (Figure 3E). The maximum enrichment factor (K_d=Q/C_e) of phenanthrene in water for the monolayer and few-layer graphene nanosheets reached 3.46×10^7. Furthermore, the facile preparation and collection of ASG make SiO_2@graphene an ideal preconcentration material for analytical chemistry, catalysis reactions and environmental pollutant management.

More surprisingly, an underlying variation in K_d/K_{HW} was observed by varying the initial concentration of phenanthrene from 5.6×10^{-3} to 5.6×10^{-6} mmol/L. A sharp peak formed in the curve of K_d/K_{HW} for the monolayer and few-layer graphene as a function of the C_e of the solute (Figures 3C and 3D), consistent with our previously reported results for the adsorption of naphthalene, phenanthrene and pyrene to pristine graphene and graphene oxide.[11] This unusual variation has not be recognized in theoretical simulations of the interaction of graphene with small organic molecules.[21] Therefore, in addition to the hydrophobic effect and π-π interactions, additional adsorption mechanisms should be considered because the actual interaction between monolayer graphene and a solute is much more complicated than previously reported. Recent studies revealed that small organic molecules will affect the morphology of graphene nanosheets.[11] Additionally, water molecules are arranged in an ice-like structure[34-37] on the liquid/solid interface of water/graphene though non-H bonding.[38] Upon interacting with low concentrations of phenanthrene, more wrinkles are generated on the extended graphene nanosheets. The ice-like water molecules attached to the flat graphene

can be replaced by phenanthrene though the replacement of the non-H bond with a stronger π-π interaction, which is a possible mechanism for increase of K_d in the low solute concentration ranges. This exchange process will reinforce the hydrophobic character of graphene, which is affected by the attachment of water molecules and the release of free energy upon phenanthrene adsorption. Thus, K_d/K_{HW} increased with C_e at low concentration ranges. The turning point of K_d/K_{HW} for ASG appeared at relatively lower C_e than that of pristine graphene. Because the monolayer and few-layer graphene nanosheets on ASG stand well in water in comparison with the piled pristine graphene, the interaction of phenanthrene with graphene nanosheets on ASG was more effective.

In summary, stable monolayer and few-layer graphene nanosheets in water were successfully prepared by a facile and low-cost method by controlling the loading of negatively charged GO on positively charged nanosilica. The true adsorption capability of monolayer and few-layer graphene nanosheets in water was reported for the first time and was extremely high compared with pristine graphene. The high efficiency and easy collection of ASG make it a promising material for the detection and treatment of environmental pollutants. Additional interaction mechanisms at the water/solid interface between monolayer graphene and organic solutes should be recognized in addition to hydrophobic effects and π-π interactions.

Electronic supplementary information (ESI) available: Experimental methods for the preparation of GO, graphene, NH_2-SiO_2, ASGO and ASG and for the adsorption experiment and characterization results including FTIR, zeta potential, Raman spectra,

element analysis, surface area and adsorption kinetics.

Acknowledgments

This project was supported by the National Science Foundation for Distinguished Young Scholars of China (Grant 2142500268), the National Basic Research Program of China (Grant 2014CB441106), the National Natural Science Foundation of China (Grants 21277120, 41071210, and 20890111).

Notes and references

1 K. S. Novoselov, A. K. Geim, S. V. Morozov, D. Jiang, Y. Zhang, S. V. Dobonos, I. V. Grigorieva, A. A. Firsov, *Science*, 2004, **306**, 666.

2 J. B. Goodenough, K. S. Park, *J. Am. Chem. Soc.*, 2013, **135**, 1167.

3 S. J. Guo, S. H. Sun, *J. Am. Chem. Soc.*, 2012, **134**, 2492.

4 H. L. Li, S. P. Pang, S. Wu, X. L. Feng, K. Mullen, C. Bubeck, *J. Am. Chem. Soc.*, 2011, **133**, 9423.

5 F. Schedini, A. K. Geim, S. V. Morozov, E. W. Hill, P. Blake, M. L. Katsnelson, K. S. Novoselov, *Nature Materials*, 2007, **6**, 652.

6 Q. F. Xia, Y. J. Huang, X. Yang, Z. Li, *Acta Chimica Sinica*, 2012, **70**, 1315.

7 O. Akhavan, E. Ghaderi, *ACS Nano*, 2010, **4**, 5731.

8 C. X. Guo, X. T. Zheng, Z. S. Lu, X. W. Lou, C. M. Li, *Adv. Mater.*, 2010, **22**, 5164.

9 K. C. Kemp, H. Seema, M. Saleh, N. H. Le, K. Mahesh, V. Chandra, K. S. Kim, *Nanoscale*, 2013, **5**, 3149.

10 L. L. Ji, W. Chen, Z.Y. Xu, S. R. Zheng, D. Q. Zhu, *J. Environ. Qual.*, 2013, **42**, 191.

11 J. Wang, Z. M. Chen, B. L. Chen, *Environ. Sci. Technol.*, 2014, **48**, 4817.

12 J. Zhao, Z. Y. Wang, Q. Zhao, B. S. Xing, *Environ. Sci. Technol.*, 2014, **48**, 331.

13 S. M. Maliyekkal, T. S. Sreeprasad, D. Krishnan, S. Kouser, A. K. Mishra, U. V. Waghmare, T. Pradeep, *Small*, 2013, **9**, 273.

14 Q. Liu, J. B. Shi, J. T. Sun, T. Wang, L. Zeng, G. B. Jiang, *Angew. Chem. Int. Ed.*, 2011, **50**, 5913.

15 Q. L. Fang, B. L. Chen, *J. Mater. Chem. A*, 2014, **2**, 8941.

16 X. T. Liu, H. Y. Zhang, Y. Q. Ma, X. L. Wu, L. X. Meng, Y. L. Guo, G. Yu, Y. Q. Liu, *J. Mater. Chem. A,* 2013, **1**, 1875.

17 G. X. Zhao, L. Jiang, Y. D. He, J. X. Li, H. L. Dong, X. K. Wang, W. P. Hu, *Adv. Mater.*, 2011, **23**, 3959.

18 H. C. Bi, X. Xie, K. B. Yin, Y. L. Zhou, S. Wan, R. S. Ruoff, L. T. Sun, *J. Mater. Chem. A,* 2014, **2**, 1652.

19 G. X. Zhao, J. X. Li, X. M. Ren, C. L. Chen, X. K. Wang, *Environ. Sci. Technol*., 2011, **45**, 10454.

20 Y. B. Sun, S. B. Yang, G. X. Zhao, Q. Wang. X. K. Wang, *Chem. Asian J*., 2013, **8**, 2755.

21 P. Lazar, F. Karlicky, P. Jurecka, K. Kocman, E. Otyepkova, K. Safarova, M. Otyepka, *J. Am. Chem. Soc.*, 2013, **135**, 6372.

22 W. S. Jr. Hummers, R. E. Offeman, *J. Am. Chem. Soc.*, 1958, **80**,1339.

23 N. I. Kovtyukhova, P. J. Ollivier, B. R. Martin, T. E. Mallouk, S. A. Chizhik, E. V. Buzaneva, A. D. Gorchinskiy, *Chem. Mater.*, 1999, **11**, 771.

24 D. Chen, H. B. Feng, J. H. Li, *Chem. Rev.*, 2012, **112**, 6027.

25 K. P. Loh, Q. L. Bao, P. K. Ang, J. X. Yang, *J. Mater. Chem.*, 2010, **20**, 2277.

26 G. Cicero, J. C. Grossman, E. Schwegler, F. Gygi, G. Galli, *J. Am. Chem. Soc.*, 2008, **130**, 1871.

27 A. C. Ferrari, J. C. Meyer, V. Scardaci, C. Casiraghi, M. Lazzeri, F. Mauri, S. Piscanec, D. Jiang, K. S. Novoselov, S. Roth, A. K. Geim, *Phys. Rev. Lett.*, 2006, **97**, 187401.

28 Z. H. Ni, Y.Y. Wang, T. Yu, Z. X. Shen, *Nano Res.*, 2008, **1**, 273.

29 M. Roos, D. Kunzel, B. Uhl, H. H. Huang, O. B. Alves, H. E. Hoster, A. Gross, R. J. Behm, *J. Am. Chem. Soc.*, 2011, **133**, 9208.

30 Z. H. Pan, N. Liu, L. Fu, Z. F. Liu, *J. Am. Chem. Soc.*, 2011, **133**, 17578.

31 M. Ishigami, J. H. Chen, W. G. Cullen, M. S. Fuhrer, E. D. Williams, *Nano Lett.*, 2007, **7**, 1643.

32 M. H. Abraham, H. S. Chadha, G. S. Whiting, R. C. Mitchell, *J. Pharmaceutical Sci.*, 1994, **83**, 1085.

33 S. Natesan, Z. B. Wang, V. Lukacova, M. Peng, R. Subramaniam, S. Lynch, S. Balaz, *J. Chem. Inf. Model.*, 2013, **53**, 1424.

34 T. O. Wehling, A. L. Lichtenstein, M. I. Katsnelson, *Appl. Phys. Lett.*, 2008, **93**, 202110.

35 O. Leenaerts, B. Partoens, F. M. Peeters, *Physical Review B.*, 2008, **77**, 125416.

36 M. I. Katsnelson, *Science*, 2010, **329**, 1157.

37 D. E. Lee, G. Ahn, S. Ryu, *J. Am. Chem. Soc.*, 2014, **136**, 6634.

38 A. Politano, A. R. Marino, V. Formoso, G. Chiarello, *Carbon*, 2011, **49**, 5180.